The 2012 World Congress on
Advances in Civil, Environmental, and Materials Research (ACEM' 12)
Seoul, Korea, August 26-30, 2012

Classification of Three-dimensional Turbulent and Transitory Flow Regimes for Inclined Circular Cylinders

*Elena Dragomirescu[1)] and Michael S. Hoftyzer[2)]

[1), 2)] *Department of Civil Engineering, University of Ottawa, Ottawa K1N 6N5, Canada*
[1)] elndrag@uottawa.ca

ABSTRACT

Several experimental and numerical investigations pointed out a possible connection between an axial flow formed on the leeward side of the inclined cables and the generation of vibrations due to dry galloping, for high Re numbers. Zdravkovich (1997) provided a comprehensive classification for flow perpendicular to the cylinders as function of the Reynolds number; however the flow regimes for the inclined and yawed cylinders were not specifically defined. In order to establish the flow regimes around inclined/yawed cylinders, a three-dimensional CFD Large Eddy Simulation has been preformed for a circular cylinder with a diameter of D = 89 mm and length of 30D, for inclinations α = 50° - 60° and yaw angles β = 0°- 40°, for Reynolds numbers Re = 1.1 – 6.7 ×10^5. Similar to the identification procedure undertaken by Zdravkovich (1997), regions of velocities higher and lower than the incoming velocity were recorded and based on the information regarding the pressure distribution, eddy viscosity and visualization of Q-criteria for the turbulence in the shear layers were used for determining the flow regimes. For most of the analyzed cases a TrSL flow regime was assigned with its variations, TrSL – Short for relative angle of attack ϕ = 53° at Re of 3.3, and 4.4 x 10^5, TrSL - Long for ϕ = 62° Re of 3.3, and 5.5 x 10^5, and TrSL – Open for ϕ = 64° at Re of 1.1 and 3.5 x 10^5 . A critical case was identified for ϕ = 60° at Re of 6.7 x 10^5 when the TrBL regime was acknowledged, similar to the ϕ = 60° at Re of 6.7 x 10^5. Axial flows were signaled on the leeward side of the cylinder for all the investigated cases, these detaching periodically as swirl threads formations.

1. INTRODUCTION

Vibrations caused by dry cable galloping, an aerodynamic phenomenon which is not completely understood, have occurred for inclined bridge cables at Re numbers of around Re = 2.2 ×10^5 (Larose et al. 2003, Cheng et al. 2008). Several wind tunnel and oil-film visualization experiments showed that the formation of an axial flow attached on

[1)] Professor
[2)] Graduate Student

the leeward side of the cable could trigger the wind-induced vibrations of the inclined cables (Matsumoto et al. 1990, Jakobsen et al. 2008, Katsuchi et al. 2009). However the exact causes of these vibrations were not yet established but suggestions were made regarding the effect of the axial flow and the dry galloping or high velocity vortex shedding phenomena. Also a possible connection between the vibrations, which occurred at high reduced wind speeds, and the coupling between the vortex shedding in the wake and along cable axis was indicated (Matsumoto 1998). Experimental studies were conducted to measure the axial flow and the velocity ratios were reported to vary from V_{axial}/U = 0.12 to 0.34 (Katsuchi et al. 2009) for a cylinder inclination of 45° and a Re= 5.0 × 10^3 or were measured on a cylinder of length 15D, where D is the diameter of the cylinder, in the range of V_{axial}/U = 0.42 to 0.78 (Matsumoto et al. 2010). Numerical investigations performed on a much longer cylinder of 30D, were in good agreement with the outcomes reported by (Matsumoto et al. 2010), namely V_{axial}/U = 0.35 to 0.6, measured at distances of 0.3D and 0.4D downstream the cylinder (Hoftyzer and Dragomirescu 2010). Verification and an interpretation of the Den-Hartog criterion adapted for inclined cables were developed by MacDonald et al. (2003).
Numerical investigations conducted for inclined cylinders for Reynolds number of 2 × 10^3 (Kawamura and Hayashi 1994) and for long inclined cylinder of lengths of 20D and 30D at high Reynolds number of 1.4 × 10^5 (Yeo and Jones 2008); these studies did not acknowledge the presence of the axial flow on the leeward side of the cylinder, however they reported other localized turbulent and rotational flow formations.
In order to clarify the flow behaviour around inclined cables, the current research employed a numerical Large Eddy Simulation (LES) investigation for very long, L = 30D, inclined and yawed cylinders, α = 50° - 60° and yaw β = 0°- 40° respectively, at high Re numbers, Re = 1.1 – 6.7 ×10^5. Initially, we focused on confirming the presence of the axial flow on the leeward side of the cylinder, and on clarifying the cable inclination and the Re numbers for which this phenomena occurs. However, after performing extensive simulations and after looking into categorizing our results within the well-known flow regime classification, provided by Zdravkovich (1997) as function of Re, we noticed that there are major differences between the wind flow mechanisms for cylinders inclined and cylinders perpendicular to the flow, for high Re numbers. Hence we report herewith the main findings, including the evolution of the velocity fields around the cylinder, the eddy viscosity, the Q-criteria turbulence visualization and the associated pressure distributions. Similarities and discrepancies with the TrBL (Transition in Boundary Layers) regime defined by Zdravkovich (1997) are discussed and new TrSL – Short – Long and –Open are assigned for the inclined cylinders.

2. NUMERICAL ALGORITHM AND MESH DETAIL

A cylinder of diameter of D = 0.089 m and a length of 30D (2.67m), inclined at angles α = 50° - 60° and yawed at β = 0°- 40° was considered as detailed in Fig 1(a). The given inclination and yaw would result in a relative angle of attack ϕ, between the cylinder and the wind direction given by Eq.1:

$$\cos\phi = \cos\alpha \cos\beta \tag{1}$$

The same settings for the inclination, yaw and relative angle of attack were used by Cheng et al. (2008) for the fixed and dynamic wind tunnel tests performed at NRC Canada, where they found that the a critical divergent vibration occurs for the cable inclined at α = 54.7° and yawed at β = 30°, (ϕ = 59.97°) and at α = 60° and yawed at β = 0 (ϕ = 60°).
The domain employed for the three-dimensional simulation had a length of 30D, width 22.5D and height 11.25D. The continuous x-component velocity for the inflow condition and advection-viscous condition for the outflow region were employed. The cylinder had the no slip, no penetration conditions, while along the walls, solely the no penetration conditions were considered. A tetrahedral mesh was used with 3092664 cells for the entire domain and a total of 666526 nodes with 247420 elements for the mesh of the cylinder (Fig.1(b)).

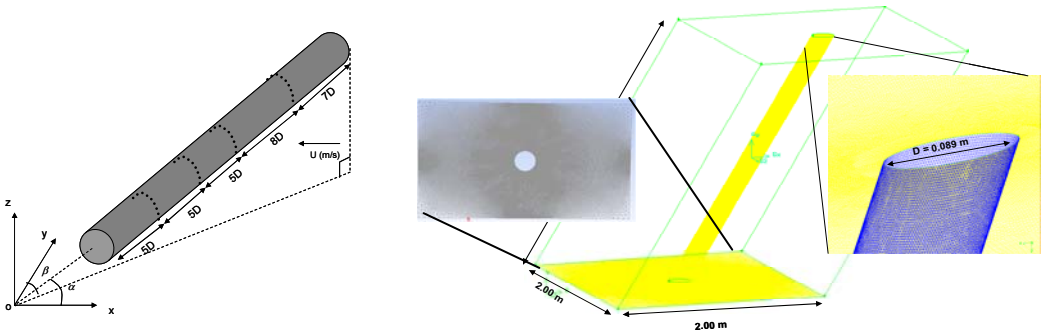

Fig. 1 Inclined Cylinder Orientation: a) Geometric dimensions, b) Mesh details

Four rings along the cylinder were monitored for pressure time histories, at 5D intervals for the first half of the cylinder and at 7D and 8D for the second half of the cylinder. Velocity vectors and streamlines visualizations were captured for middle rings of the cylinder and eddy viscosity profiles were presented as a characteristic of the turbulence around the cylinder. High Reynolds numbers of Re = 1.1×10^5 to 6.7×10^5, corresponding to wind speeds for of 8.6 m/s to 57 m/s, were used. LES algorithm with the Smagorinsky-Lilly algorithm for the eddy viscosity at subgrid-scale were employed through a commercial software for the wind flow simulation. The advection term in non-dimensional Navier-Stokes equations was discretized with the finite difference method (FDM) and was solved through a second-order implicit time integration. Spatial discretization was estimated through the second-order upwind scheme and the diffusion term in the transport equation was discretized through central-differenced method. A Smagorinsky constant of C_s = 0.1 was considered and the non-dimensional time step Δt was set to 0.01.

2. FLOW MECHANISM FOR INCLINED CYLINDERS

The classification of the flow regimes for one cylinder, perpendicular to the flow, provided by Zdravkovich (1997), which compiles extensive data from several researchers, is mainly conducted based on the flow visualization in one plane and is reporting the averaged pressure coefficient at the circumference of the cylinder. Several flow regimes were identified in regard with the above mentioned data spanning

from laminar regime for low Re numbers of 0 to 180-200, transition in wake regime (TrW) for Re = 180-200 to 350-400, transition in shear layers regime (TrSL) for Re = 350-400 to 1.0 - 2.0×10^5 and transition in boundary layers (TrBL) for Re = 1.0 - 2.0×10^5 to more than 6.0×10^6. The higher the Re number the more difficult capturing the flow pattern around cylinders perpendicular to flow is achieved, due to the limited dimensions of the experimental facilities and the turbulent conditions of the flow.
For inclined cylinders however, the flow mechanism is different and flow visualization in one plane does not suffice for a complete description of the regime, but a three-dimensional representation is required.

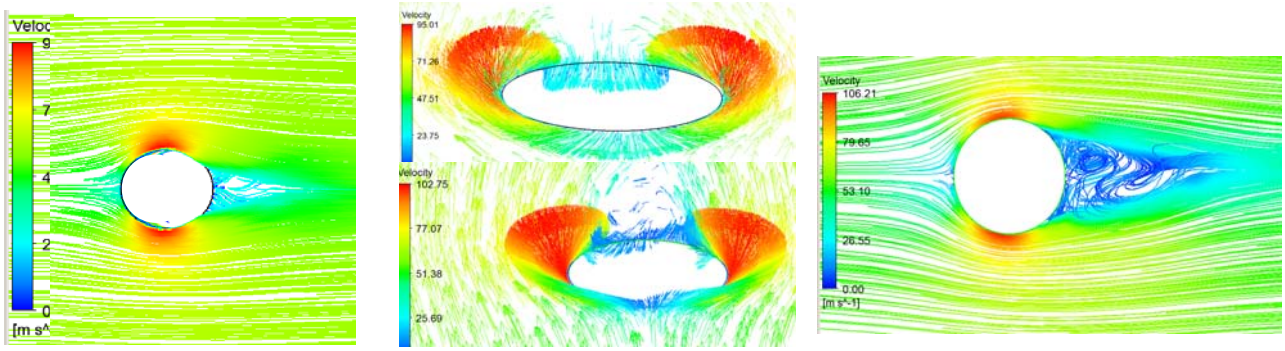

Fig. 2 Velocity streamlines and vectors distribution for Re = 6.7 x 10^5 for a) ϕ = 60° and b,$_{up}$) ϕ = 60°, b,$_{down}$) ϕ = 0° and c) ϕ = 0°

The velocity streamlines in the plane of the middle ring on the cylinder which is inclined to the flow with ϕ = 60° measured at Re = 6.7 x 10^5 has shown a very smooth flow pattern, with shear layers uniformly surrounding the cylinder until its leeward side (Fig. 2 (a)), where these detach from its surface and seemed to converge towards a joining point downstream the cylinder. The vectors of the velocity however indicated that after detachment the streamlines would actually change their direction on the leeward side, moving downwards, along the cylinder and not downstream (Fig. 2 (b,$_{up}$)). For the cylinder perpendicular to the flow, at same Re = 6.7 x 10^5, it could be noticed that the streamlines will keep their parallel tracks until the detachment points sidewise the cylinder, from where these will depart downstream with the flow; however behind the cylinder and in the immediate vicinity of its leeward surface, there was an alternate vortices formation (Fig. 2 (c)), also pointed out by the velocity vectors which had opposite directions in that region, indicating that part of the streamlines would go upwards the cylinder and part of them would go downstream the cylinder (Fig. 2 (b,$_{down}$)). Because it was still unclear the volume of flow which will have an in-plane evolution, and the flow which will be re-directed along the cylinder, as an axial flow, a three-dimensional visualization of the captured streamlines in regard to the cylinder was shown in Figs. 3.
For the flow perpendicular on the cylinder, the wind streamlines would move along one single plane until encountering the cylinder, then after the contact these will be deviated,

developing into a turbulent formation behind the cylinder which will continue to move along the downstream direction of the flow, not in the same plane as the initial flow, but not necessarily on a different direction (Fig. 3 (a)). For the flow inclined to the cylinder at ϕ = 60°, was obvious that the wind streamlines will disrupt their path after the impact with the cylinder and will stream along the cylinder axis, on its leeward side forming a slightly undulated axial flow (Fig. 3 (b)). However these will gradually detach from the cylinder, at lower points, and will travel downstream (Fig. 3 (c)). The in-plane movement will be encountered only for the streamlines which are not in the vicinity of the cylinder.

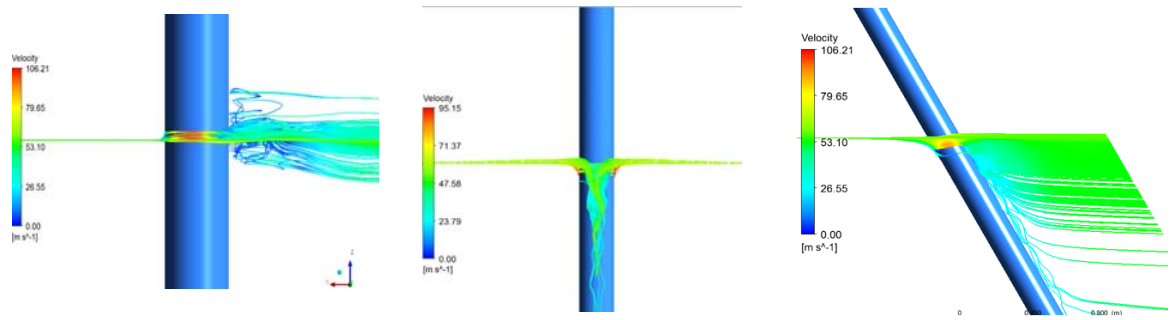

Fig. 3 Three-dimensional flow visualization, velocity streamlines for Re = 6.7 x 10^5 for a) ϕ = 0°, b) ϕ = 60°, front view and c) ϕ = 60°, side view

Hence, the major difference between the flow mechanisms for cylinders inclined at ϕ = 0° and at ϕ = 60° consists in the change of direction of the streamlines, which remained attached to the cylinder for ϕ = 60°, and streamed along its axis on the leeward side, forming an axial flow which detaches periodically from the cylinder. Therefore we could say that the axial flow which was signalled in experiments by several researchers (Matsumoto 1998, Jakobsen et al. 2008, Cheng et al. 2008, Katsuchi et al. 2009) is not a localized flow pattern, but is a characteristic of the flow regime for inclined cylinders. The effect on the pressure distribution and velocity streamlines for other cases will be detailed below, for a better description of the flow regime for inclined cylinders.

3. CLASIFFICATION OF THE FLOW REGIMES FOR INCLINED CYLINDERS

The identification of flow patterns and regimes were conducted by observing several parameters, such as pressure, velocity and eddy viscosity distributions and by acknowledging the flow regions where the velocity increased or decreased compared with the input velocity, V_0. A close comparison with the regimes identified by Zdravkovich (1997), for flow perpendicular to cylinders, was followed and main similarities and disparities were pointed out in the figures below.

3.1. *Two-dimensional velocity profiles and disturbed flow zones*

Several cases were investigated for different inclinations α = 50° - 60° and yaw angles of β = 0° - 40°, for Re numbers of 1.1 to 6.7 x 10^5, however for maintaining the

consistency of the results the relative angle of attack ϕ was reported. Commencing with a similar delimitation of velocity fields, as the one used by Zdravkovich (1997) for

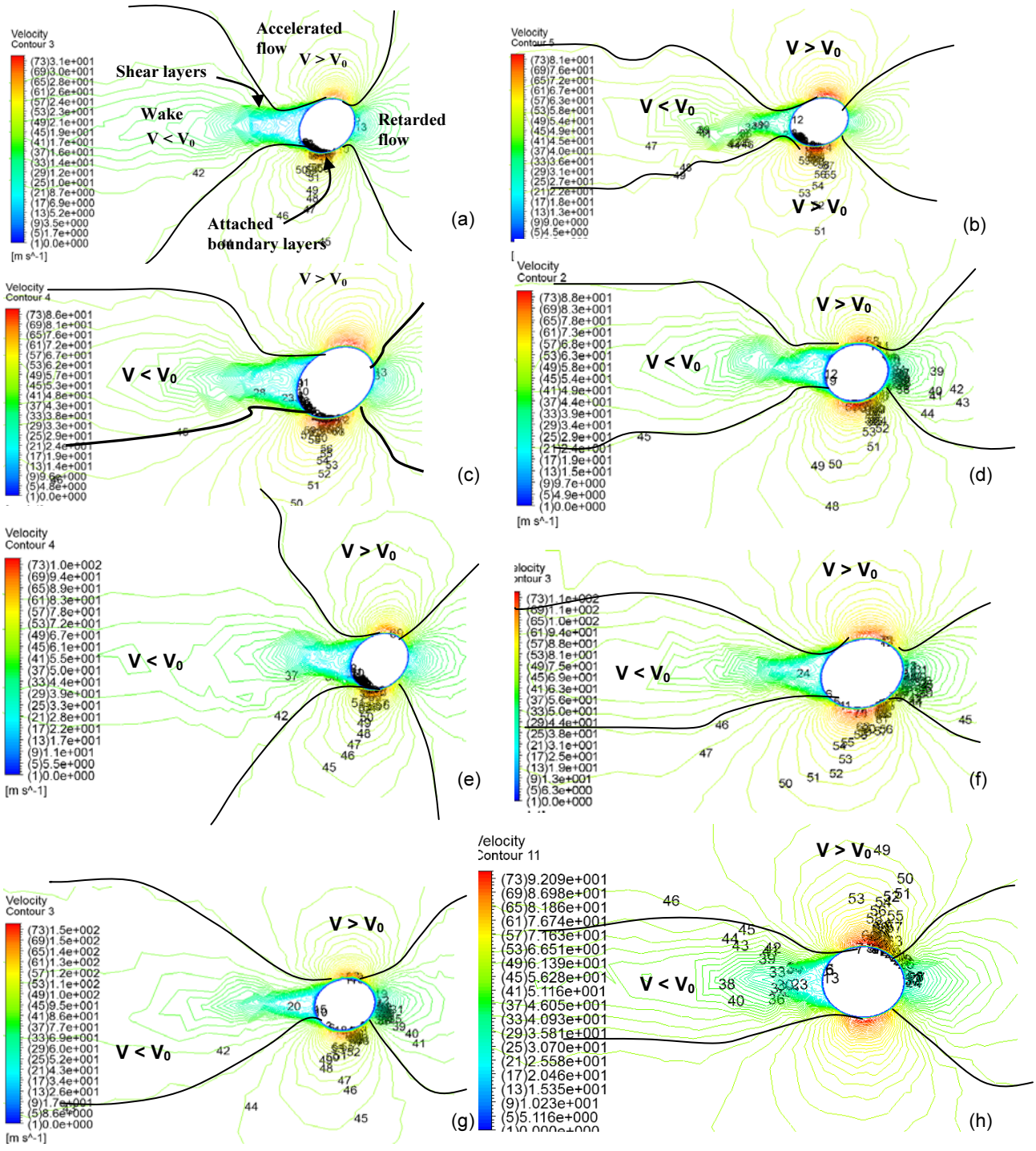

Fig. 4 Dominant velocity zones and flow pattern for a) ϕ = 64°, Re 1.1 x 10^5, b) ϕ = 53°, Re 3.3 x 10^5 c) ϕ = 60.5°, Re 3.3 x 10^5 d) ϕ = 62°, Re 3.3 x 10^5e) ϕ = 64°, Re 3.5 x 10^5 f) ϕ = 53°, Re 4.4 x 10^5 g) ϕ = 62°, Re 5.5 x 10^5 and h) ϕ = 60°, Re 6.7 x 10^5

defining the regions of retarded flow, the boundary layers attached to the surface of the cylinder, which will develop into free shear layers, the regions of displaced and accelerated flow, sidewise the cylinder and the downstream region of separated flow or the wake.
For the inclined cylinders investigated herewith, was noticed that all the above mentioned flow characteristics and the disturbed flow regions will be encountered, however, the retarded flow region at the incoming flow, is not as narrow as for the case of the flow perpendicular to the cylinder (Zdravkovich, 1997), contrary this region is as wide as the wake region downstream the cylinder, for most of the cases. The difference might be caused by the broad simulation domain used in our analysis, compared with the limited sampling points and streamline dye techniques used for the flow visualization in the wind tunnel experiments.
For the simplicity of the picture, the zones of retarded, accelerated, wake flow and the location of the boundary and shear layers were detailed only for Fig. 4 (a), for the rest of the cases, Figs. 4 (b) – (h), only the representation by lines the relationship between the velocities being adopted. Relative angles of attack between ϕ = 53° and 64° were investigated for Re up to 6.7 x 10^5. It was notice that the inclination would have a dominant effect upon the flow pattern namely, for higher angles of attack, ϕ = 64° both the retarded and the wake flow regions had a very wide width, regardless of the Re number (Fig. 4 (a) and (e)), while the shear layers shedding from the cylinder and forming a long and open wake behind the cylinder. For lower angles of ϕ = 62°, the retarded and wake regions were not very wide, leaving more space for the accelerated flow regions on the two sidewise of the cylinder (Fig. 4 (d) and (g)). Moreover the wake formed behind the cylinder had a sharp, long shape, the shear layers meeting at around 1D distance downstream the cylinder. The lowest angles of attack ϕ = 53° (Fig. 4 (b) and (f)) had the retarded and wake regions of medium width, but the wake behind the cylinder was sharp and short, with shear layers intersecting each other at around 0.5D downstream the cylinder. For the case of ϕ = 60.5° (Fig. 4 (c)) the flow pattern had a similar evolution as for the ϕ = 64°, however the ϕ = 60° case showed a very abrupt and short wake behind the cylinder, the streamlines meeting in the vicinity of the leeward side of the cylinder (Fig. 4 (h)).
As a feature of flow around bluff bodies, the earlier researches (Roshko and Fiszdon, 1969) indicated that the transition from laminar to turbulent flow, with the increase of the Re number, will take place gradually, first with a transition in the wake (TrW) then a transition in the shear layers (TrSL) and then a transition in the boundary layers (TrBL). Based on the Figs 4 (a) – (h) we could determine the transition regions given the intensities of the flow velocity, however no concrete information regarding the turbulence encountered in the wake, shear layers and the boundary layer was provided. Hence the eddy viscosity around the cylinder was presented in Figs. 5 below.

3.2. Transition to turbulent shear layers and turbulent boundary layer

There are numerous turbulence properties, such as turbulence intensity, Monin-Obukov length, Kolmogorov wavelength, turbulent kinetic energy k, turbulent dissipation ε, etc., which are equally used by structural and mechanical engineers for characterizing the turbulence in atmospheric boundary layer. In the current research, the Large Eddy Simulation (LES) was employed as a turbulence model and two-

dimensional eddy viscosity profiles along with three dimensional Q-criterion velocity gradient method was used for determining the regions where the rotational formations of the fluid dominates over the strain rate.

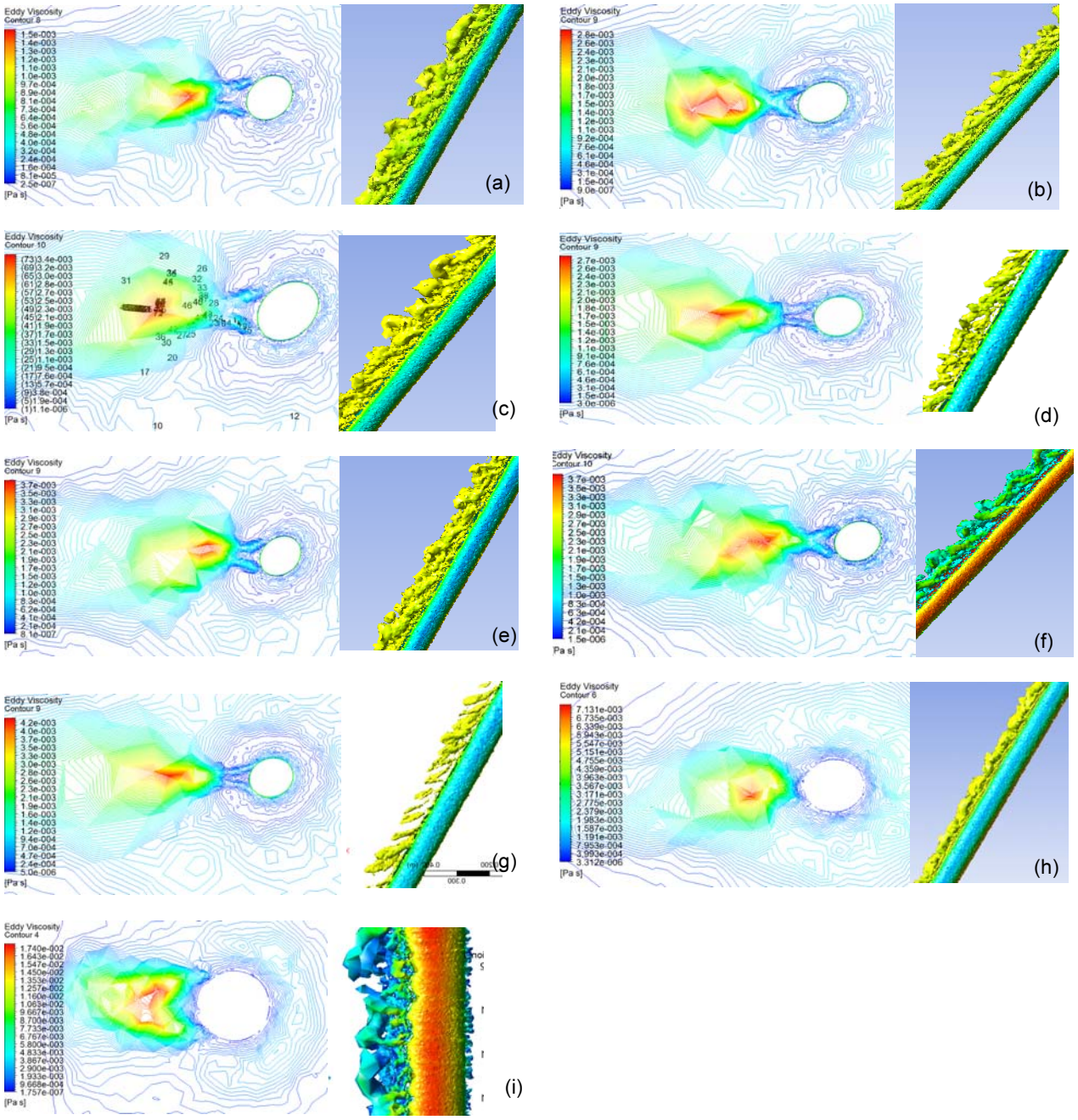

Fig. 5 Two-dimensional eddy viscosity profiles and associated three-dimensional visualization of the Q-criterion for a) ϕ = 64°, Re 1.1 x 10^5, b) ϕ = 53°, Re 3.3 x 10^5 c) ϕ = 60.5°, Re 3.3 x 10^5 d) ϕ = 62°, Re 3.3 x 10^5 e) ϕ = 64°, Re 3.5 x 10^5 f) ϕ = 53°, Re 4.4 x 10^5 g) ϕ = 62°, Re 5.5 x 10^5 h) ϕ = 60°, Re 6.7 x 10^5 and i) ϕ = 0°, Re 6.7 x 10^5

The two-dimensional eddy viscosity pattern has pointed out that turbulence in the shear layers would occur, and intensive turbulent formations were formed in the wake region, not very far from the cylinder. Also, the three-dimensional velocity field given by the Q-criterion as explained above has shown that a change in direction of the wind flow occurred, and threads of swirl flow were encountered along the leeward side of the cylinder, moving as an axial flow along its axis and not along the wind initial direction (Figs. 5 (a) to (i)). Depending on the relative angle of attack and the Re number, was noticed that length of the generated swirl threads and the wakes in the two-dimensional profiles varied and that the distance the swirl threads of turbulent flow will detach from the cylinder in the three dimensional profiles also varied, as described below.

For lower relative angles of attack of $\phi = 53°$, for both Re = 3.3 x 10^5 and Re = 4.4 x 10^5, two turbulent shear layers detached from the cylinder, intersecting each other downstream very close to the cylinder, and generating a main turbulent wake at around 0.5D downstream the cylinder (Figs. 5 (b) and (f)). The three-dimensional profiles associated with the same figures showed long, intermittent swirl threads of flow, streaming downstream the leeward side of the cylinder and detaching from it at periodic intervals. For the $\phi = 62°$, at Re = 3.3 x 10^5 and Re = 5.5 x 10^5, the flow around the cylinder manifested a similar behavior, however turbulent shear layers were longer and intersected each other at about 1D downstream the cylinder, as it can be noticed in Figs. 5 (d) and (g). Also the three-dimensional visualization showed similar swirl threads which will stream along the cylinder, however these will detach much earlier from its surface. For the highest relative angles of attack of $\phi = 64°$, at Re = 1.1 x 10^5 and Re = 3.5 x 10^5, Figs. 5 (a) and (e) the turbulent shear layers had more space between them at detachment such that a space was formed behind the cylinder, before reaching the turbulent wake downstream. The swirl threads were similar as for the $\phi = 62°$ case, with an earlier detachment from the leeward side of the cylinder.

There was a transition of flow regimes between the $\phi = 60.5°$ at Re = 3.3 x 10^5 and $\phi = 60°$ at Re = 6.7 x 10^5, Figs. 5 (c) and (h) respectively, which might be caused by the higher Re more than the inclination angle as follows: the first case encountered short turbulent shear layers shedding from both sides of the cylinder, which intersected and formed a turbulent wake downstream the cylinder, which is represented by the short flow threads visualized in the three-dimensional detail of the eddy viscosity profile; for the case of $\phi = 60°$ at Re = 6.7 x 10^5, the turbulent flow formed on the leeward of the cylinder, with no turbulent shear layers and actually a swirly undulated flow could be noticed attached to the cylinder, and streaming along its axis, without detaching towards the downstream flow, as for the rest of the cases.

Also, it was observed that for the standard case of $\phi = 0°$, the eddy viscosity indicated the occurrence of turbulent wake in the immediate vicinity of the leeward side of the cable, hence the shear layers which are shed from the cylinder engulfed the turbulent wake (Fig. 5 (i)), which was in conformity with the TrBL2 regime identified by Zdravkovich (1997). The visual information extracted from the analytical simulation did not show any shear layer reattachment, hence a discussion regarding the formation for the separation bubbles was not made and the general TrBL notation was used instead of the detailed TrBL2 or TrBL3 as categorized by Zdravkovich (1997). Actually the cylinder inclined with $\phi = 60°$, (Fig. 5 (h)) presented a very similar flow pattern, with turbulent wake directly attached to the cable's leeward side, which is actually caused by

the axial flow indicated in the Fig. 3 (c). It should be mentioned that the wind tunnel tests performed by various researchers (Matsumoto 1998, Jakobsen et al. 2008, Cheng et al. 2008, Katsuchi et al. 2009) have indicated a critical vibration for the same case of ϕ = 60°, at high Re numbers and a possible connection with the occurrence of an axial flow on the leeward side of the cable.

Based on the velocity profiles described in Figs. 4 (a) – (h) and the eddy viscosity and swirl threads formations presented in Figs. 5 (a) – (i) we could suggest three flow regimes for the inclined cylinders analysed herewith, which are a combination of the TrSL and TrBL regimes:

- TrSL – Short and Long (Figs. 5 (b), (f) and (c), (d), (g) respectively): when the major axis of the ellipse (the cross-section of the inclined cable) is close to the horizontal and the turbulent shear layers detach almost on the leeward side of the cylinder but they intersect immediately after at 0.5D (TrSL-Short) or at 1D from the cylinder (TrSL-Long), forming a turbulent wake downstream; It is applicable for Re of 3.3 to 4.4 x 10^5 and for ϕ = 53°, and for Re of 3.3 to 5.5 x 10^5 for ϕ = 62°. Schematic representation of TrSL – Short and Long can be found in Figs. 6 (a) and (b).
- TrSL – Open (Fig. 5 (a) and (e)): when the major axis of the ellipse is closer to the vertical and the shear layers detach sidewise from the cylinder for Re of 1.1 to 3.5 x for ϕ = 64°. TrSL – Open was represented in Fig. 6 (c).
- TrBL (Fig. 5 (d)): when the transition to turbulent regime is in the boundary layer surrounding the cylinder and the turbulent wake forms from in the immediate vicinity of the leeward side of the cylinder. This was noticed for Re of 6.7 x 10^5 for ϕ = 0°, and also for the critical case of ϕ = 60°. Schematic representation of TrBL was done in Figs. 6 (d).

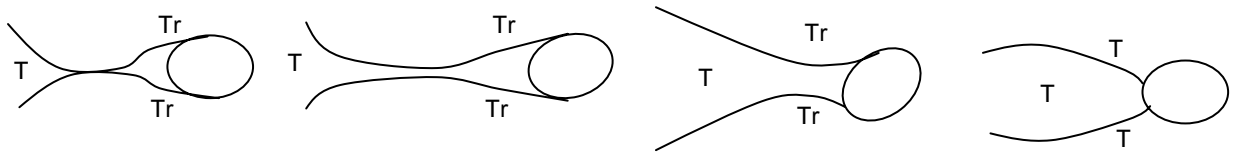

Fig. 6 Flow regimes for inclined cylinders a) TrSL-Short, b) TrSL – Long, c)TrSL – Open and d) TrBL (T = Transition, Tr = Trubulent)

Is worth mentioning that the free shear layers detaching from the inclined cylinders do not have a similar development as the shear layers Zdravkovich (1997) presented in the flow regime classification for the cylinders perpendicular to flow, where these always detached symmetrically, from the sideways of the cylinder and engulfed the wake region. In the present case, the shear layers will detach at various locations at the circumference of the ellipse, sometimes not symmetric and in most of the cases the turbulent wake will be formed after their intersection downstream the cylinder.

4. PRESSURE DISTRIBUITON AROUND INLCINED CYLINDERS

For flow perpendicular to the cylinder Zdravkovich (1997) showed that the pressure

coefficient (Cp) distribution will vary with the increase of Re number, namely the minimum value of the Cp will decrease and its position will move along the circumference of the cylinder towards downstream. The separation (inflection) point will also move towards downstream, shifting its position with up to 17° (Fig. 7 (a)). For the inclined cylinders investigated in the current research, the relative angle of attack had more influence upon the variation of the values and distribution of Cp, than the Re numbers. Also the pressure distribution was not symmetric around the cylinder as it would be for the flow perpendicular to the cable, due to the elliptic shape of the cross section, hence the entire distribution was plotted in Fig. 7 (b).

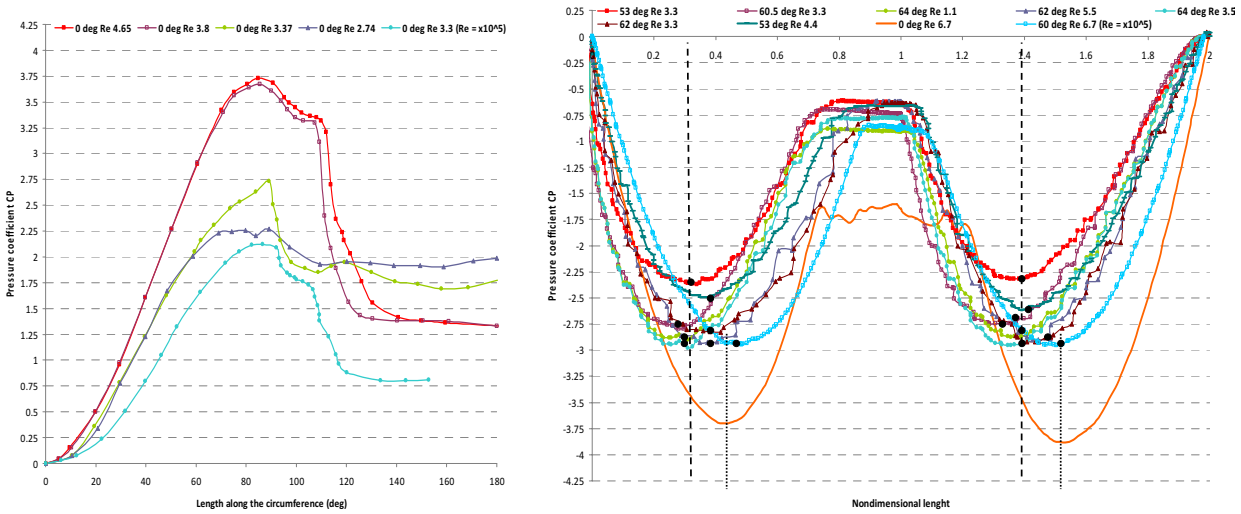

Fig. 7 Pressure coefficient for a) ϕ = 0° at Re 2.74 to 4.65 x 10^5 from Zdravkovich (1997) b) ϕ = 53° to 64° at Re 1.1 to 6.7 x 10^5, current study

The minimum value of pressure coefficient was between Cp = -2.25 and -2.5 for ϕ = 53°, Cp = -2.75 and -3.0 for ϕ = 60°, 62° and 64° Fig. 7 (b). In general, with the increase of the Re number to up to 6.7 x 10^5 the pressure coefficient decreased. Also the position of the minimum pressure points and the separation points changed slightly towards the leeward side of the cylinder, with the increase of Re number, however the change was not very significant, hence we could conclude that there was no change in the flow regime, and all the cases followed the TrSL regime, with the exception of ϕ = 60°, at Re 6.7 x 10^5 as it can be noticed in Fig. 7 (b). For this critical case, the shape of the pressure coefficient distribution is different from the previous cases, the minimum pressure point shifting its position towards the leeward side of the ellipse on one branch but slightly towards the upwind side on the other branch and was almost aligned with the position of the minimum pressure coefficient registered for ϕ = 0°, at Re = 6.7 x 10^5.

CONCLUSION

Inclined and yawed cylinders were analyzed for α = 50° - 60° and yaw β = 0°- 40° respectively, which were converted to relative angles of attack of ϕ = 53° to 64°, for different Reynolds numbers of Re = 1.1 to 6.7 x 10^5. Pressure, velocity fields and eddy

viscosity distribution along with Q-criteria turbulence patterns were monitored around the cylinders for determining the evolution of the flow regimes for inclined and yawed cylinders, and were compared with the standard case of ϕ = 0° and the flow regimes defined by Zdravkovich (1997).

Major differences between the cylinder perpendicular to the flow and cylinder inclined in regard to the flow direction were noticed, namely, shear layers will shed from the leeward side of the cylinder towards a turbulent wake, for the inclined cylinders, compared with the shear layers shed from the sideways of the cylinder and surrounding the turbulent wake formed behind it, for the cables perpendicular to the flow. The detached shear layers will intersect each other at various distances behind the cylinder 0.5 D, 1.0 D, depending on the relative angle of attack ϕ = 53° and 62° at Re of 1.1, 3.3 and 5.5 x 10^5 such that a TrSL-Short and TrSL-Long flow regimes were assigned; a turbulent wake formed beyond these distances. A TrSL-Open was assigned for the case where the shear layers don't meet downstream (ϕ = 64°, Re of 3.5 x 10^5), but shed towards a turbulent wake formation further into the downstream flow. Also, for the inclined cylinders the flow on the leeward side of the cylinder changed its direction and streamed along the axis of the cable, detaching periodically from the cylinder, as swirl threads. A critical case was identified for the ϕ = 60° at Re of 6.7 x 10^5 when shear layers detached from the sidewise of the cylinder and enveloped the turbulent wake formed behind the cylinder, flow characteristics which are very similar to the TrBL regime defined by Zdravkovich (1997) for the flow perpendicular to cylinders, and which was also noticed in the current investigation for ϕ = 0° at Re of 6.7 x 10^5. A difference however was noticed in the axial flow which streamed along the cylinder axis on its leeward side for ϕ = 60° and it detaches periodically as undulated swirls and not threads as for the other cases of inclined cylinders. The pressure coefficient distribution showed very similar evolution for all the investigated cases, with small variations of the position of the minimum pressure and detachment points along the circumference of the cylinder, which has an ellipse as a cross-section due to the inclinations, proving that there was no change in the flow regime TrSL, but just variations within the same regime TrSL – Open, - Short and – Long. It must be mentioned that the TrSL – Open, - Short and - Long regimes characterized in the present article are not identical with the TrSL regimes defined in Zdravkovich (1997), the position of the turbulent shear layers and the turbulent wake pattern having a different configuration. For the critical case of ϕ = 60° at Re of 6.7 x 10^5 the evolution along the cylinder circumference of the pressure coefficient was shifted towards the leeward side of the cylinder, actually having a very similar shape, but different magnitudes, with the pressure coefficient evolution for ϕ = 0° at Re of 6.7 x 10^5 proving that the same TrBL flow regime is registered for these two cases.

REFERENCES

Zdravkovich, M. M. (1997), "Flow around Circular Cylinders Vol 1: Fundamentals" First Edition, Oxford University Press, New York, NY, USA.

Cheng, S., Larose, G.L., Savage, M.G., Tanaka, H., Irwin, P.A., (2008), "Experimental study on the wind-induced vibration of a dry inclined cable—Part I: Phenomena", *J. Wind Eng. Ind. Aerodyn.,* **96**(12): 2231-2253.

FHWA/HNTB, (2005), "Wind induced vibration of stay cables", Interim final report, RDT 05-004.

Hoftyzer, M.S., and Dragomirescu, E., (2010) “Numerical investigation of flow behaviour around inclined circular cylinders”, *Proc. Of 5th Intl. Symp on Computational Wind Engineering*, Chapel Hill, NC, USA .
Katsuchi, H. and Yamada, H., (2009), “Surface pressure and axial flow measurements for indented-surface stay cable”, *Proc. of 8th Intl. Symp on Cable Dynamics*, Paris, France, 215 - 222.
Kawamura, T., Hayashi, T., (1994), “Computation of flow around a yawed circular cylinder”, Japan Society of Mechanical Engineers International Journal, Series B, **37**(2), 229–236.
Larose, G.L., Savage, M.G., Jakobsen, J.B., (2003), “Wind tunnel experiments on an inclined and yawed circular cylinder in the critical Reynolds number range”, Proceedings of the 11th Intl Conf on Wind Engineering, Lubbock, TX, pp. 1705–1712.
Matsumoto, M., Shiraishia, N., Kitazawab, M., Kniselya, C., Shiratoa, H., Kimc, Y., Tsujiia, M., (1990), “Aerodynamic behaviour of inclined circular cylinders-cable aerodynamics”, *J. Wind Eng. Ind. Aerodyn.,* **33** (1-2), 63-72.
Matsumoto, M., Yagi, T., Hatsuda, H., Shima, T., Tanaka, M., Naitoa, H., (2010), “Dry galloping characteristics and its mechanism of inclined/yawed cables”, *J. Wind Eng. Ind. Aerodyn.,* **98** (6-7): 317-327.
Macdonald, J.H.G., and Larose, G.L., (2003), “Two-degree-of-freedom inclined cable galloping—Part 1: General formulation and solution for perfectly tuned system”, *J. Wind Eng. Ind. Aerodyn.,* **96** (3): 291-307.
Macdonald, J.H.G., and Larose, G.L., (2006), “A unified approach to aerodynamic damping and drag\lift instabilities, and its application to dry inclined cable galloping”, J. of Fluid. Struct. **22**(2): 229-252.
Roshko, H., and Fiszdon, W., (1969), “On the persistence of transition in the near-wake” Problems in Hydrodynamics and Continuum Mechanics, Philadelphia, SIAM, 606-16.
Saito, T., Matsumoto, M., Kitazawa, M., (1994), “Rain-wind excitation of cables on cable- stayed Higashi-Kobe Bridge and cable vibration control”, Proc. of the Int. Conf. A.I.P.C.-F.I.P. Cable-Stayed and Suspension Bridges, 507–514.
Scruton, C., and Newberry, C.W., (1963), “On the estimation of wind loads for building and structural design”, Proc. Institution of Civil Engineers. **25**: 97–126.
Simiu, E., Scanlan, R.H., (1987), “Wind Effect on Structures”, 1st Ed., John Wiley & Sons, New York, NY, USA.
Yeo, D., and Jones, N.P., (2008), “Investigation on 3-D characteristics of flow around a yawed and inclined circular cylinder”, *J. Wind Eng. Ind. Aerodyn.,* **96**(10-11): 1947-1960.
Zdravkovich, M. M., (1997), “Flow around Circular Cylinders Vol 1: Fundamentals”, 1st Ed., Oxford University Press, New York, NY, USA.